

Epitaxial growth of ultrathin gallium films on Cd(0001)

Zuo Li(李佐), Mingxia Shi(石明霞), Gang Yao(姚钢), Minlong Tao(陶敏龙), and Junzhong Wang(王俊忠)
Citation: Chin. Phys. B, 2024, 33 (**1**): 018101. DOI: 10.1088/1674-1056/acfb7a
Journal homepage: http://cpb.iphy.ac.cn; http://iopscience.iop.org/cpb

What follows is a list of articles you may be interested in

Molecular dynamics study of thermal conductivities of cubic diamond, lonsdaleite, and nanotwinned diamond via machine-learned potential

Jia-Hao Xiong(熊佳豪), Zi-Jun Qi(戚梓俊), Kang Liang(梁康), Xiang Sun(孙祥), Zhan-Peng Sun(孙展鹏), Qi-Jun Wang(汪启军), Li-Wei Chen(陈黎玮), Gai Wu(吴改), and Wei Shen(沈威)
Chin. Phys. B, 2023, 32 (**12**): 128101. DOI: 10.1088/1674-1056/ace4b4

Activated dissociation of H_2 on the Cu(001) surface: The role of quantum tunneling

Xiaofan Yu(于小凡), Yangwu Tong(童洋武), and Yong Yang(杨勇)
Chin. Phys. B, 2023, 32 (**10**): 108103. DOI: 10.1088/1674-1056/acd2b3

Enhanced xylene sensing performance of hierarchical flower-like Co_3O_4 via In doping

Jing Zhang(张京), Jianyu Ling(凌剑宇), Kuikun Gu(谷魁坤), Georgiy G. Levchenko, and Xiao Liang(梁霄)
Chin. Phys. B, 2023, 32 (**6**): 068104. DOI: 10.1088/1674-1056/acbe30

Suppression and compensation effect of oxygen on the behavior of heavily boron-doped diamond films

Li-Cai Hao(郝礼才), Zi-Ang Chen(陈子昂), Dong-Yang Liu(刘东阳), Wei-Kang Zhao(赵伟康),Ming Zhang(张鸣), Kun Tang(汤琨), Shun-Ming Zhu(朱顺明), Jian-Dong Ye(叶建东),Rong Zhang(张荣), You-Dou Zheng(郑有炓), and Shu-Lin Gu(顾书林)
Chin. Phys. B, 2023, 32 (**3**): 038101. DOI: 10.1088/1674-1056/ac7f8a

Edge-and strain-induced band bending in bilayer-monolayer Pb_2Se_3 heterostructures

Peng Fan(范朋), Guojian Qian(钱国健), Dongfei Wang(王东飞), En Li(李恩), Qin Wang(汪琴), Hui Chen(陈辉), Xiao Lin(林晓), and Hong-Jun Gao(高鸿钧)
Chin. Phys. B, 2021, 30 (**1**): 018105. DOI: 10.1088/1674-1056/abcf92

Epitaxial growth of ultrathin gallium films on Cd(0001)

Zuo Li(李佐)[1,2], Mingxia Shi(石明霞)[1], Gang Yao(姚钢)[1], Minlong Tao(陶敏龙)[1], and Junzhong Wang(王俊忠)[1,†]

[1] *School of Physical Science and Technology, Southwest University, Chongqing* 400715, *China*
[2] *School of Science, Guizhou University of Engineering Science, Bijie* 551700, *China*

(Received 18 July 2023; revised manuscript received 17 September 2023; accepted manuscript online 20 September 2023)

Growth and electronic properties of ultrathin Ga films on Cd(0001) are investigated by low-temperature scanning tunneling microscopy (STM) and density functional theory (DFT) calculations. It is found that Ga films exhibit the epitaxial growth with the pseudomorphic 1×1 lattice. The Ga islands deposited at 100 K show a ramified shape due to the suppressed edge diffusion and corner crossing. Furthermore, the majority of Ga islands reveal flat tops and a preferred height of three atomic layers, indicating the electronic growth at low temperature. Annealing to room temperature leads to not only the growth mode transition from electronic growth to conventional Stranski–Krastanov growth, but also the shape transition from ramified islands to smooth compact islands. Scanning tunneling spectroscopy (STS) measurements reveal that the Ga monolayer exhibits metallic behavior. DFT calculations indicate that all the interfacial Ga atoms occupy the energetically favorable hcp-hollow sites of the substrate. The charge density difference analysis demonstrates that the charge transfer from the Cd substrate to the Ga atoms is negligible, and there is weak interaction between Ga atoms and the Cd substrate. These results shall shed important light on fabrication of ultrathin Ga films on metal substrates with novel physical properties.

Keywords: gallium films, electronic growth, STM/STS, density functional theory

PACS: 81.15.–z, 73.20.At, 68.37.Ef, 82.20.Wt **DOI:** 10.1088/1674-1056/acfb7a

1. Introduction

In heteroepitaxial systems, growth of thin films on solid substrates offers the opportunity to create new structures (thin-film phases) that do not exist in the bulk phases.[1] Serving as the metastable structures, these new phases may exhibit novel physical and chemical properties. In the process of epitaxial growth, elastic strain arising from the lattice mismatch greatly influences the growth mode of thin films.[2] When the lattice misfit is low, the elastic strain energy can be accommodated in the form of pseudomorphic growth, where the thin films adopt the same lateral periodicity as the substrate.[3–5] At higher lattice misfit, the strain energy is relieved by the formation of misfit dislocations at the film/substrate interface.

The trivalent metal gallium, a liquid metal near room temperature, plays a crucial role in the electronic and optoelectronic devices.[6] In the past decades, the heteroepitaxial thin films of gallium grown on solid surfaces have attracted considerable interest. The Ga bilayer grown on GaN(0001) exhibits a pseudomorphic 1×1 structure and reveals superconductivity with the transition temperature of 5.4 K.[7,8] Furthermore, the quantum Griffiths singularity was observed in this Ga bilayer.[9] Recently, ultrathin gallium films, also known as gallenene, have received considerable interests due to the potential application in the emerging elemental 2D materials.[10–20] By means of solid-melt exfoliation, Kochat *et al*. fabricated the atomically thin gallium films, i.e., gallenene sheets, on silicon substrates.[10] Tao *et al*. realized the epitaxial growth of gallenene monolayer on the Si(111)-$\sqrt{3} \times \sqrt{3}$-Ga template.[11] Ultra-thin Ga islands, analogues of high pressure Ga(Ⅲ), was found on the Si(111) surface.[14] In particular, gallenene sheets with thickness of one to three atomic layers were intercalated at the interface between epitaxial graphene and silicon carbide through confinement heteroepitaxy.[16] Interestingly, the Ga sheets can be regarded as 'half van der Waals' metal, because they are covalently bonded to the SiC below but present a non-bonded interface to the graphene overlayer.

In this work, we utilize the hexagonal close-packed metal Cd(0001) thin films as substrates to grow 2D Ga sheets. Compared to the noble metals Au, Ag and Cu, the metal Cd possesses a smaller electronegativity and negative electron affinity.[21,22] Consequently, charge transfer effect between the Ga atoms and Cd(0001) films is expected to be very weak. It is found that the first atomic layer of Ga deposited on Cd(0001) surface forms the pseudomorphic 1×1 phase. Depending on the substrate temperature, Ga films consist of either fractal island when deposited at a low temperature (100 K), or compact islands after room-temperature annealing. Further increasing the Ga coverage leads to Ga multilayers with the pseudomorphic 1×1 lattice. Scanning tunneling spectroscopy (STS) measurements demonstrate that Ga monolayer exhibits metallic behavior. Density functional theory (DFT) calculations indicate that the hcp-hollow site of Cd(0001) is the most energetically favorable site of Ga atoms.

†Corresponding author. E-mail: jzwangcn@swu.edu.cn

© 2024 Chinese Physical Society and IOP Publishing Ltd

2. Methods

2.1. Sample preparation and characterizations

The experiments were performed in a Unisoku low temperature STM system with the base pressure less than 2.0×10^{-10} Torr. The clean Si(111)-7×7 surface was prepared by flashing the sample to $\sim$ 1500 K for several seconds. A smooth Cd(0001) thin film of 15 monolayers (ML) was obtained by depositing Cd atoms on the Si(111)-7×7 surface at room temperature. Ga atoms were thermally sublimated from a boron nitride crucible heated to 930 K. During the deposition of Ga atoms, the temperature of Cd(0001) substrate was kept at $\sim$ 100 K. An electrochemically etched tungsten tip after electron-beam heating was utilized for STM imaging. STS measurements were performed with the lock-in technique by applying a small modulation of 20 mV to the applied voltage at 373 Hz at 77 K. The STM images were analyzed using Gwyddion software.[23]

2.2. Density functional theory calculations

Optimization of geometric structures has been calculated using the generalized gradient approximation (GGA) of Perdew–Burke–Ernzerhof formula[24] and the norm-conserving Vanderbilt pseudopotentials[25] within the QUANTUM ESPRESSO package.[26] The slab model was constructed by consisting of Ga atomic layers, six Cd atomic layers, and a vacuum layer of 20 Å was inserted to avoid the coupling between atomic layers along the c axis. After the convergence test, the kinetic-energy cutoff and the charge-density cutoff were chosen to be 60 Ry and 480 Ry, respectively. The charge densities were calculated on an unshifted mesh of $17 \times 17 \times 2$ points in combination with a marzari-vanderbilt smearing of 0.02 Ry.[27] The geometry optimization was performed until all components of all forces became less than 1×10^{-4} Ry/Bohr. Based on the optimized structure, we carried out band structure calculations.

3. Results and discussion

We utilized the smooth Cd(0001) films as the substrate to grow the ultrathin Ga films. Figure 1(a) show the morphology of the as-grown Cd(0001) films with a thickness of 15 ML. The smooth Cd(0001) films show flat terraces ($\sim$ 200 nm width). The height profile along the blue line in panel (a) reveals a step height of 2.8 ± 0.1 Å in Fig. 1(b), which is consistent with the interlayer spacing of bulk Cd along the [0001] direction.[21] From the high-resolution STM image in Fig. 1(c), the in-plane structure of Cd(0001) films exhibits a hexagonal lattice constant of $c_0 = 3.0 \pm 0.1$ Å, also consistent with that (0001) plane of bulk Cd. Figure 1(d) shows the atomic model of Cd(0001) films, where four high-symmetric sites are marked as FCC (FCC-hollow), HCP (HCP-hollow), bridge, and top, respectively.

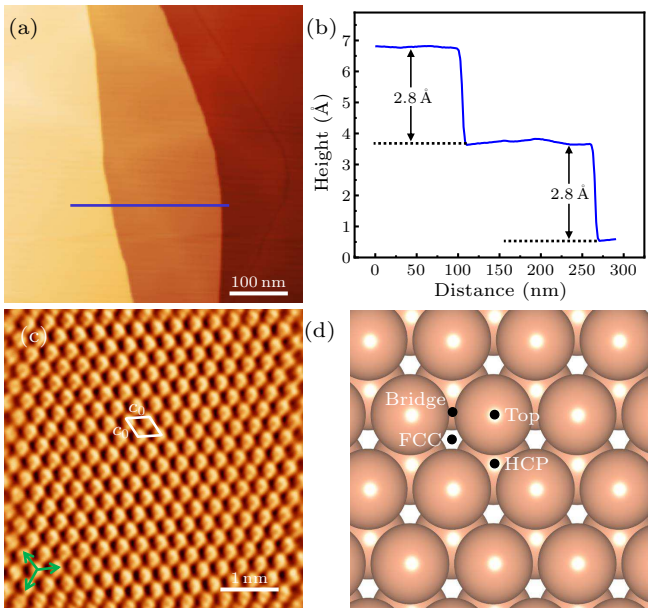


Fig. 1. (a) Large-scale STM image of the Cd(0001) thin film grown on Si(111)-7×7 ($U = 3.0$ V, $I_t = 20$ pA). (b) Height profile along the blue line in panel (a), showing the step height of 2.8 ± 0.1 Å. (c) High-resolution STM image of the Cd(0001) thin film showing a hexagonal lattice ($U = 0.65$ V, $I_t = 35$ pA). (d) Atomic model of the Cd(0001) surface. light Orange balls represent Cd atoms. The high-symmetric sites are marked as FCC (FCC-hollow), HCP (HCP-hollow), bridge, and top.

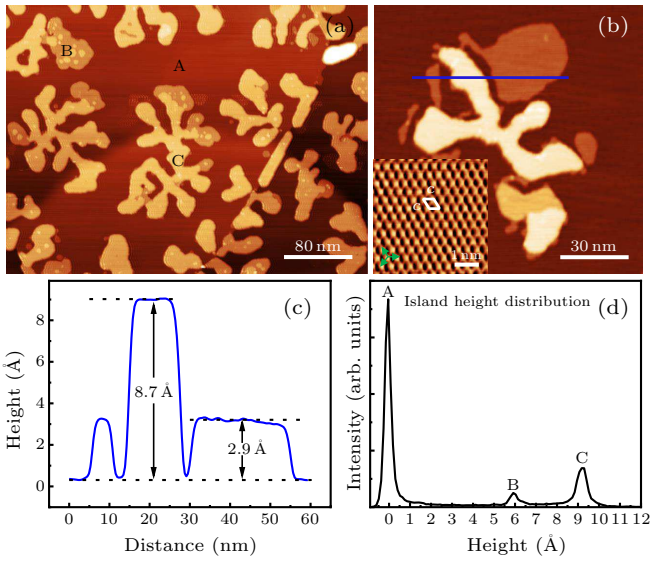


Fig. 2. Low-temperature growth of Ga sheets on Cd(0001). (a) Ramified Ga islands formed on the Cd(0001) surface at 100 K ($\Theta = 0.7$ ML, $U = 2.0$ V, $I_t = 20$ pA). (b) Close-up view of a ramified Ga island and several small Ga islands ($U = 0.9$ V, $I_t = 20$ pA). Inset: the atomic-resolution STM image of monolayer Ga island ($U = 0.35$ V, $I_t = 20$ pA). (c) Height profile along the blue line in (b) showing the apparent heights of a ramified Ga island and compact Ga islands. (d) Height distribution of the Ga islands appearing in the upper terrace of (a), showing two preferred heights (B and C peaks).

Firstly, we studied the low-temperature growth of Ga sheets on Cd(0001). In the submonolayer regime, 0.7 ML of Ga atoms was deposited onto the Cd(0001) surface, which was kept at $\sim$ 100 K. It was observed that the Ga atoms aggregate into large ramified islands with flat tops, as shown Fig. 2(a). Nearby the substrate steps there exist several stripe-like Ga islands. Based on the nucleation and aggregation theory, the

formation of ramified islands with fractal-like shape can be attributed to the suppressed edge diffusion and corner crossing of adatoms around an island.[2] However, close inspection of the island shapes indicates that the islands exhibit a large branch width ($\sim$ 20 nm). Furthermore, the primary branch edges are rather smooth without sub-branches. It means that the deposition temperature of 100 K is not low enough to completely inhibit the edge diffusion and corner crossing of Ga adatoms.

From the close-up view in Fig. 2(b), it is observed that the ramified Ga islands consist of branches with different heights. The highest branches show a height of 8.7 ± 0.1 Å, while the lowest branches have a height of 2.9 ± 0.1 Å [Fig. 2(c)], corresponding to three-layer and monolayer of Ga, respectively. From the height distribution shown in Fig. 2(d), it can be found that the flat-top Ga islands have two preferred heights of 5.6 ± 0.2 Å (peak B) and 8.9 ± 0.2 Å (peak C), corresponding to two and three layers of Ga, respectively. Among these Ga islands, those of three-layer height are the most abundant. We notice that this growth mode is similar to the previous 'electronic growth' mode observed in the Pb and Ag films grown on Si(111) or GaAs.[28–30] The mechanism of electronic growth is attributed to the competition between quantum size effect in the metal films and charge transfer occurring at the interface.[31]

The inset of Fig. 2(b) is a high-resolution STM image of the monolayer Ga island. It exhibits a hexagonal lattice with periodicity of 3.0 ± 0.1 Å, which is identical to the lattice of Cd(0001) surface. It means that the first Ga layer is pseudomorphic to the Cd(0001) substrate. The elastic strain energy arising from lattice misfit is accommodated by the pseudomorphic 1×1 structure. Moreover, we noticed that the second layer and third layer of ramified Ga islands also reveal the pseudomorphic 1×1 structure.

Annealing the low-temperature deposited Ga films (0.5 ML) to room temperature leads to formation of compact Ga islands, as shown in Fig. 3(a). It is found that the compact islands are hundreds of nanometers in size, and the island edges are very smooth but not straight. The shape change from the small fractal-like island to large compact island can be attributed to the coalescence and reshaping of the small ramified islands in the process of island merging. Moreover, we notice a striking phenomenon that most of the compact Ga islands show the thickness of a single atomic layer, and only a few islands are two atomic layers thick. As shown in Fig. 3(b), the compact Ga islands still maintain the pseudomorphic 1×1 structure as in the case of ramified islands. At the high coverage regime (1.1 ML), as shown in the STM images of Fig. 3(c), the first-layer islands show a compact shape with smooth edges, the second-layer islands appear on top of the first layer. When the Ga coverage is increased to 2.5 ML, both the second-layer islands and third-layer islands appear simultaneously on top of the first layer, as shown in Fig. 3(d). It was also observed that the third Ga layer still show the same pseudomorphic 1×1 lattice as the first and second Ga layers.

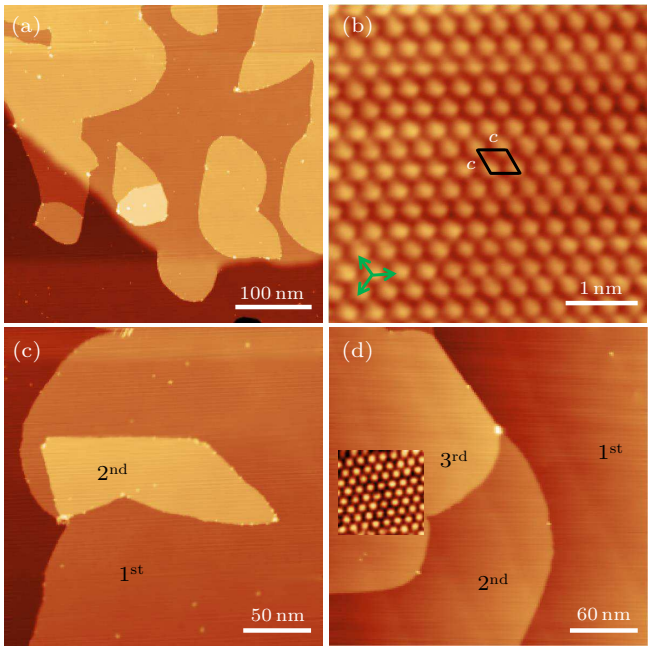


Fig. 3. Formation of compact Ga islands after room-temperature annealing. (a) STM image of the compact Ga islands formed on Cd(0001) surface ($\Theta = 0.5$ ML, $U = 2.0$ V, $I_t = 20$ pA). (b) Atomic-resolution STM image of the monolayer Ga island ($U = 0.35$ V, $I_t = 20$ pA). (c) Morphology of 1.1 ML of Ga sheets formed on Cd(0001), ($U = 1.5$ V, $I_t = 20$ pA). (d) Topographic image of 2.5 ML of Ga sheets grown on Cd(0001), ($U = 2.0$ V, $I_t = 20$ pA). Inset: the pseudomorphic 1×1 structure observed in the third layer of Ga (2.5 nm $\times$ 2.5 nm, 0.5 V, 25 pA).

These results mean that room-temperature annealing leads to the transition from electronic growth to conventional SK growth, implying that the observed electronic growth at a low temperature is metastable against the thermal annealing. We notice that such metastability of electronic growth was also observed in the Ag films grown on Si(111), where the plateau islands evolve into huge mounds and pyramids upon annealing to 450 K.[28]

In Table 1, we summarize the reported lattice constants of monolayer Ga grown on different substrates. It can be found that the Ga films prefer to adopt the same periodicity as the substrates, i.e., pseudomorphic phase, when grown on GaN(0001) and Cd(0001), or intercalated between SiC and graphene. On the other hand, it can be found that the in-plane lattice constants of Ga sheets can be varied significantly from 2.72 Å to 3.18 Å. In addition, the adsorption height between 2D Ga monolayer and substrate surfaces is closed to the interlayer height of the GaN(0001), SiC(0001), and Cd(0001) substrates, respectively. Hence, the substrate structures play a crucial role for the epitaxial growth of Ga films.

We perform DFT calculations for the adsorption energy of Ga monolayer on the Cd(0001) surface to get insight into the experimental results. The adsorption energy E_{ads} is used

to evaluate the strength of the adsorbate-substrate interaction. Herein, E_{ads} is defined as the mean adsorption energy per adatom,

$$E_{ads} = [E_{Ga/Cd(0001)} - nE_{Ga} - E_{Cd(0001)}]/n, \quad (1)$$

where $E_{Ga/Cd(0001)}$ and $E_{Cd(0001)}$ represent the total energy of the Cd(0001) surface after and before Ga adatoms adsorption; n is the number of adatom; and E_{Ga} is the energy of an isolated Ga atom. According to the definition, the negative value of the adsorption energy represents exothermic, and vice versa. In order to determine the most stable adsorption sites of Ga atoms, relative location models, which are denoted by top, bridge, FCC-hollow, and HCP-hollow sites, have been established for computing the lowest adsorption energy of system. After all geometries have been optimized, the calculated results are shown in Table 2. All energies of four adsorption sites are negative, in particular, the hcp-hollow site is the most energetically favorable site for Ga atom on Cd(0001) because of the adsorption energy of about −0.4 eV. The calculated lattice constant of the 2D Ga layer ($c = 2.99$ Å) and the adsorption height ($h = 2.68$ Å) are in good agreement with the experimental results. Additionally, the calculated Ga–Ga bond length of 2D Ga (2.99 Å) is closed to that of γ-Ga crystal (2.90 Å).[32]

Table 1. Lattice constants of 2D Ga grown on different substrates.

Substrate	Lattice constants of substrate (Å)	Lattice constants of Ga monolayer (Å)	Height of Ga adatom on surface (Å)	Interlayer height of substrate (Å)
GaN(0001)[a]	3.19	3.18	2.76	2.67
SiC(0001)[b]	2.70	2.72	3.10	3.10
Cd(0001)	3.01	3.01	2.90	2.80

[a]Ref. [8], [b]Ref. [16].

Table 2. Summary of the calculated Ga adsorption energies, lattice constants (c) of Ga monolayer and height of Ga adatom (h) for the different sites of the Cd(0001) surface.

Sites	E_{ads} (eV)	h (Å)	c (Å)
Top	−0.316	2.93	2.99
Bridge	−0.393	2.70	2.99
FCC-hollow	−0.384	2.71	2.99
HCP-hollow	−0.399	2.68	2.99

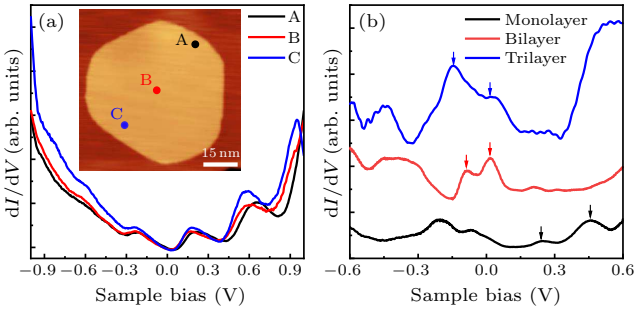


Fig. 4. Differential conductance spectra acquired in Ga film. (a) Three differential tunneling conductance (dI/dV) spectra ($U = 0.5$ V, $I_t = 170$ pA) acquired at different positions of the monolayer Ga island: island short-edge (A), island center (B), and island long-edge (C), respectively. Inset: STM image of monolayer Ga island where STS spectra were acquired ($U = 1$ V, $I_t = 20$ pA). (b) The evolution of dI/dV spectra with layer thickness. Monolayer ($U = 0.5$ V, $I_t = 170$ pA), bilayer ($U = 0.8$ V, $I_t = 150$ pA), trilayer ($U = 0.5$ V, $I_t = 370$ pA).

We carry out the STS measurement on top of a monolayer Ga island (Fig. 4(a)) to derive the electronic properties of the Ga sheets. Three differential tunneling conductance (dI/dV) spectra are recorded at different sites of the island: island short-edge (A), island center (B), and island long-edge (C), respectively, as shown in Fig. 4(a). All spectra include the two peaks at −0.21 eV and +0.2 eV around Fermi level (E_F), reflecting spatial homogeneity of the electronic states. A V-type dip is always observed in the energetic range of −0.21 eV to 0.2 eV, similar to the STS spectra of the high pressure Ga(Ⅲ) (001) surface.[14] The evolution of dI/dV spectra with layer thickness is shown in Fig. 4(b). The STS of Ga monolayer is influenced by the Cd(0001) substrate, which appears the characteristic peak (black arrow) of substrate.[21] However, the STS of bilayer exists the Ga characteristic peak (red arrow) near Fermi level, indicating a weaker influence from substrate. As the Ga films become three layers, this peak moves towards the low energy (blue arrow). These results are consistent with DFT calculations.

In order to gain insight into the electronic properties of Ga atomic layers on Cd(0001), the band structures are computed using DFT, as illustrated in Fig. 5(a). According to the pseudomorphic relationship between the lattices of monolayer Ga and the Cd(0001) substrate, the high-symmetry points Γ, M, and K are chosen for describing the energy band properties of hexagonal lattice, resembling to that of Ga atomic layers on SiC(0001).[16] Obviously, the energy bands from monolayer to trilayer become steeper and steeper, indicating the delocalization enhancement of Ga electrons in the thicker film. The contribution of Ga atoms to band structure becomes dominating. This thickness-dependent behavior can be confirmed by the enlarged intensities of local density of states near E_F. Furthermore, to understand the charge transfer between Ga atomic layers and Cd(0001) surface, the charge density difference is calculated based on the geometry optimization. The charge density displacement ($\Delta\rho(\boldsymbol{r})$) induced by the adatom adsorption is analyzed:

$$\Delta\rho(\boldsymbol{r}) = \rho_{ads/sur}(\boldsymbol{r}) - \rho_{ads}(\boldsymbol{r}) - \rho_{sur}(\boldsymbol{r}), \quad (2)$$

where $\rho_{ads/sur}$ is the charge density of the adsorbate system, ρ_{ads} is the charge density of the isolated adlayer, and ρ_{sur} is the charge density of the clean surface. As shown in Fig. 5(b), most of the charge accumulation appears in the interface region between Ga and Cd atomic layers, with a small amount dispersed between Ga adatoms due to the interfacial Coulomb repulsion for monolayer Ga. The charge accumulation of interface region decreases, as the number of Ga layers increases. In order to further illustrate charge distribution, planar average of the charge density displacement for Ga/Cd(0001) system along z axis is displayed in Fig. 5(c). The largest change in the electron density distribution occurs in the interface between Ga adatoms and the Cd(0001) surface, resembling the results of the charge density difference. Thus, the charges of $0.033e$, $0.031e$, and $0.013e$ are transferred to Ga monolayer, bilayer, and trilayer, respectively. It is revealed that the interfacial charge transfers contribute to the electronic growth of Ga films.

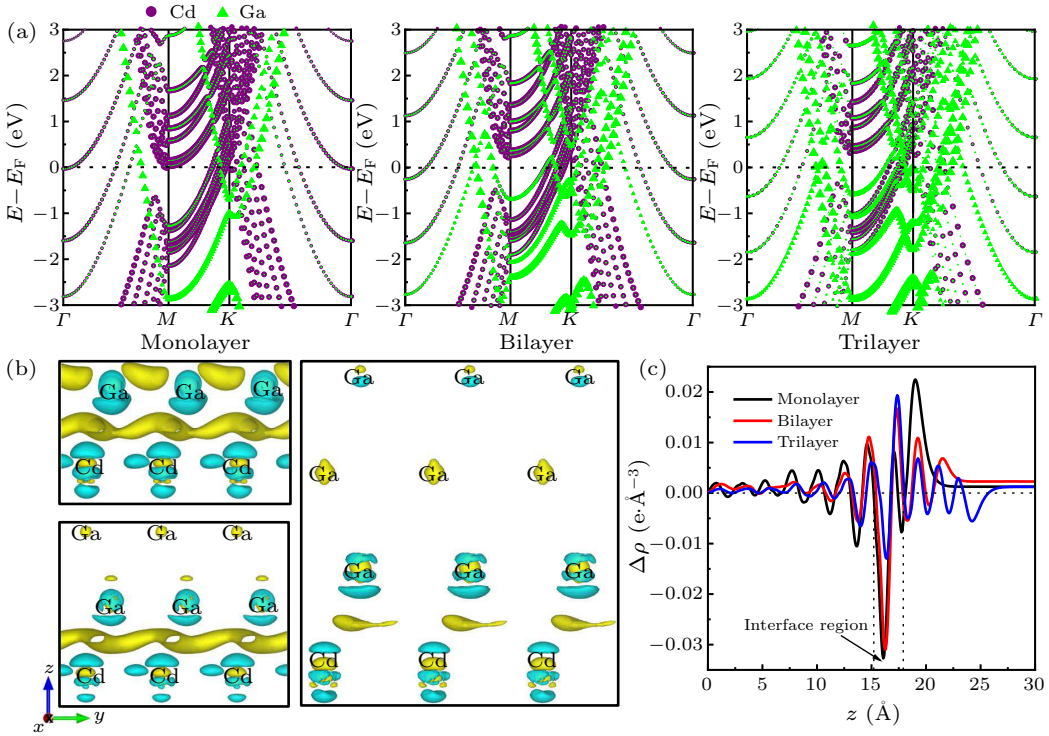


Fig. 5. (a) The contribution of each atom in the band structure. The purple circle and green triangle indicate the contribution of Cd and Ga atoms, respectively. The size of the symbols represents the strength of the contribution. The Fermi level is set to be zero energy. (b) Side view of charge density differences with iso-surface value of 1.5×10^{-3} e/Bohr^3 of Ga atomic layers on Cd(0001). Yellow and blue regions indicate charge accumulation and depletion, respectively. (c) Planar average of the charge density displacement for Ga/Cd(0001) system.

4. Conclusion

In summary, pseudomorphic growths have been observed in the monolayer, bilayer, and trilayer of Ga sheets on Cd(0001). Depending on the substrate temperature, Ga islands have a ramified shape at low temperature, and a compact shape after room-temperature annealing. Ga islands reveal a preferred three atomic layer at a low coverage, which implies that the formation of Ga islands follows the electronic growth. Moreover, the room-temperature annealing leads to the transition from electronic growth to conventional SK growth. DFT calculations demonstrate that all the interfacial Ga atoms occupy the energetically favorable hcp-hollow sites of the substrate. STS and DFT calculations demonstrate the metallic nature of Ga monolayer. The charge is transferred from the Cd(0001) surface to the Ga atomic layers, revealing that the interfacial charge transfers contribute to the electronic growth of Ga films. Our finding sheds important light on fabrication of ultrathin Ga films on metal substrates with novel physical properties.

Acknowledgement

Project supported by the National Natural Science Foundation of China (Grant Nos. 11874304 and 11574253).

References

[1] Venables J A, Spiller G D T and Hanbucken M 1984 *Rep. Prog. Phys.* **47** 399
[2] Brune H 1998 *Surf. Sci. Rep.* **31** 125
[3] Arthur J R 2002 *Surf. Sci.* **500** 189
[4] Hahn E, Kampshoff E, Wälchli N and Kern K 1995 *Phys. Rev. Lett.* **74** 1803
[5] Pratzer M, Elmers H J and Getzlaff M 2003 *Phys. Rev. B* **67** 153405
[6] Moskalyk R R 2003 *Miner. Eng.* **16** 921
[7] Northrup J E and Neugebauer J 2000 *Phys. Rev. B* **61** 9932

[8] Zhang H M, Sun Y, Li W, Peng J P, Song C L, Xing Y, Zhang Q, Guan J, Li Z, Zhao Y, Ji S, Wang L, He K, Chen X, Gu L, Ling L, Tian M, Li L, Xie X C, Liu J, Yang H, Xue Q K, Wang J and Ma X 2015 *Phys. Rev. Lett.* **114** 107003

[9] Xing Y, Zhang H M, Fu H L, Liu H, Sun Y, Peng J P, Wang F, Lin X, Ma X C, Xue Q K, Wang J and Xie X C 2015 *Science* **350** 542

[10] Kochat V, Samanta A, Zhang Y, Bhowmick S, Manimunda P, Asif S A S, Stender A S, Vajtai R, Singh A K, Tiwary C S and Ajayan P M 2018 *Sci. Adv.* **4** 1701373

[11] Tao M L, Tu Y B, Sun K, Wang Y L, Xie Z B, Liu L, Shi M X and Wang J Z 2018 *2D Mater.* **5** 035009

[12] Badalov S V, Yagmurcukardes M, Peeters F M and Sahin H 2018 *J. Phys. Chem. C* **122** 28302

[13] Steenbergen K G and Gaston N 2019 *Chem. Commun.* **55** 8872

[14] Li Y, Zhang J, Yin F, Wang Y, Feng H, Zhou S and Du Y 2019 *Nanoscale* **11** 17201

[15] Nakhaee M, Yagmurcukardes M, Ketabi S A and Peeters F M 2019 *Phys. Chem. Chem. Phys.* **21** 15798

[16] Briggs N, Bersch B, Wang Y, Jiang J, Koch R J, Nayir N, Wang K, Kolmer M, Ko W, De La Fuente Duran A, Subramanian S, Dong C, Shallenberger J, Fu M, Zou Q, Chuang Y W, Gai Z, Li A P, Bostwick A, Jozwiak C, Chang C Z, Rotenberg E, Zhu J, van Duin A C T, Crespi V and Robinson J A 2020 *Nat. Mater.* **19** 637

[17] Petrov M, Bekaert J and Milošević M V 2021 *2D Mater.* **8** 035056

[18] Lambie S, Steenbergen K G and Gaston N 2021 *Nanoscale Adv.* **3** 499

[19] Wundrack S, Momeni D, Dempwolf W, Schmidt N, Pierz K, Michaliszyn L, Spende H, Schmidt A, Schumacher H W, Stosch R and Bakin A 2021 *Phys. Rev. Mater.* **5** 024006

[20] Kutana A, Altalhi T, Ruan Q, Zhang J J, Penev E S and Yakobson B I 2022 *Nanoscale Adv.* **4** 1408

[21] Tao M L, Xiao H F, Sun K, Tu Y B, Yuan H K, Xiong Z H, Wang J Z and Xue Q K 2017 *Phys. Rev. B* **96** 125410

[22] Lineberger W C 1976 *IEEE Trans. Nucl. Sci.* **23** 934

[23] Nečas D and Klapetek P 2012 *Cent. Eur. J. Phys.* **10** 181

[24] Perdew J P, Burke K and Ernzerhof M 1996 *Phys. Rev. Lett.* **77** 3865

[25] Hamann D R 2013 *Phys. Rev. B* **88** 085117

[26] Giannozzi P, Baroni S, Bonini N, Calandra M, Car R, Cavazzoni C, Ceresoli D, Chiarotti G L, Co-coccioni M, Dabo I, Dal Corso A, De Gironcoli S, Fabris S, Fratesi G, Gebauer R, Gerstmann U, Gougoussis C, Kokalj A, Lazzeri M, Martin-Samos L, Marzari N, Mauri F, Mazzarello R, Paolini S, Pasquarello A, Paulatto L, Sbraccia C, Scandolo S, Sclauzero G, Seitsonen A P, Smogunov A, Umari P and Wentzcovitch R M 2009 *J. Phys.: Condens. Matter* **21** 395502

[27] Marzari N, Vanderbilt D, De Vita A and Payne M C 1999 *Phys. Rev. Lett.* **82** 3296

[28] Gavioli L, Kimberlin K R, Tringides M C, Wendelken J F and Zhang Z Y 1999 *Phys, Rev. Lett.* **82** 129

[29] Su W B, Chang S H, Jian W B, Chang C S, Chen L J and Tsong T T 2001 *Phys. Rev. Lett.* **86** 5116

[30] Yu H, Jiang C S, Wang X D, Niu Q, Shih C K, Ebert P, White J M, White J M, Shih C K, White J M, Niu Q, Shih C K and Zhang Z Y 2002 *Phys. Rev. Lett.* **88** 016102

[31] Zhang Z Y, Niu Q and Shih C K 1998 *Phys. Rev. Lett.* **80** 5381

[32] Bosio L, Curien H, Dupont M and Rimsky A 1972 *Acta Crystallogr. Sect. B* **28** 1974